REPORT DOCUMENTATION PAGE

AFRL-SR-AR-TR-04-

0345

1. AGENCY USE ONLY *(Leave blank)*	2. REPORT DATE	3. REPORT TYPE AND DATES COVE...
	November 2003	Final Technical Report 1 Apr 98 - 30 Sep 01

4. TITLE AND SUBTITLE
PROBABILISTIC SIMULATION OF FATIGUE CRACK INITIATION

5. FUNDING NUMBERS
F49620-98-1-0401
2302/BS
61102F

6. AUTHOR(S)
Anthony Ingraffea

7. PERFORMING ORGANIZATION NAME(S) AND ADDRESS(ES)
Cornell University
Hollister Hall
Ithaca, NY 14853

8. PERFORMING ORGANIZATION REPORT NUMBER

9. SPONSORING/MONITORING AGENCY NAME(S) AND ADDRESS(ES)
AFOSR/NA
4015 Wilson Blvd., Room 713
Arlington, VA 22203-1954
Dr. Thomas Kim

10. SPONSORING/MONITORING AGENCY REPORT NUMBER

11. SUPPLEMENTARY NOTES

12a. DISTRIBUTION AVAILABILITY STATEMENT
APPROVED FOR PUBLIC DISTRIBUTION, DISTRIBUTION UNLIMITED

12b. DISTRIBUTION CODE

13. ABSTRACT *(Maximum 200 words)*

Final Progress (1 Apr 98 - 30 Sep 01):
Many fatigue-related studies have been conducted on the workhorse alloys for airframe construction over the past 20-30 years. The body of empirical knowledge related to establishing relationships between loading conditions and fatigue life or fatigue crack growth rates, including environmental effects is vast. One consistent observation is that the number of cycles it takes to initiate a fatigue crack (imitation life) in high strength aluminum alloys, like AA 7075, is a significant fraction of total life. Fundamental understanding of what causes fatigue cracks to initiate is elusive, however, and current alloy and airframe component design methodologies remain highly empirical processes.

14. SUBJECT TERMS			15. NUMBER OF PAGES
			16. PRICE CODE: 46
17. SECURITY CLASSIFICATION OF REPORT: U	18. SECURITY CLASSIFICATION OF THIS PAGE: U	19. SECURITY CLASSIFICATION OF ABSTRACT: U	20. LIMITATION OF ABSTRACT

2-19-04 8-4-04

Table of Contents

1.0 INTRODUCTION

Many fatigue-related studies have been conducted on the workhorse alloys for airframe construction over the past 20-30 years. The body of empirical knowledge related to establishing relationships between loading conditions and fatigue life or fatigue crack growth rates, including environmental effects is vast (c.f. [1] [2] [3] [4] [5] [6]). One consistent observation is that the number of cycles it takes to initiate a fatigue crack (initiation life) in high strength aluminum alloys, like AA 7075, is a significant fraction of total life. Fundamental understanding of what causes fatigue cracks to initiate is elusive, however, and current alloy and airframe component design methodologies remain highly empirical processes.

The focus of this project was on the initiation of fatigue microcracks in aluminum alloys like AA 7075. The objective was the creation of a simulation methodology for representing the structure of a polycrystalline metal and its evolution during processing and service conditions. At the heart of this methodology was a construction called *Digital Material.* From the Digital Material (DM) one can generate virtual samples of a material that reflect the distributions of grain sizes, crystallographic orientations, precipitate densities etc., which are observed experimentally in physical samples of that material. Once generated, a sample can be characterized and loaded with simulation tools that are closely analogous to the techniques employed by the experimentalist to investigate the actual material. The formulation is multiscale, experimentally-motivated, and probabilistic in nature. The overall goal of this research was the creation of the DM environment, which included a multiscale material representation and the virtual tools necessary to construct specimens and to characterize their microstructure. Those specimens could then be tested by simulation under cyclic loading to

understand and predict the initiation of fatigue cracks in AA 7075. The schematic depiction of the DM is in Figure 1.

This report details the development and testing of the key elements of the DM environment. Section 2 describes material features and attributes accommodated by the DM. Section 3 describes sample generation and probe tools. Section 4 describes material evolution tools, and their probabilistic bases.

2.0 DIGITAL MATERIAL: GEOMETRICAL FEATURES AND ATTRIBUTES

At the core of the Digital Material lie geometrical features that define the microstructure (grains, particles, dislocations ...) and the statistical distributions of attributes that are associated with those features. Experimental data, drawn from either physical or numerical sources, define the geometries and their attributes. Attributes of geometrical feature at one length scale often are used to synthesize other geometrical features at finer scales. They may also be used to compute properties over an ensemble. An example is the orientation of the crystallographic lattice. Its distribution is the texture, which is an attribute of the grains of a polycrystal and can be used to determine the macroscopic yield surface. At a finer scale, one can assign specific lattice orientations to individual grains or even construct an atomic lattice using samples draw from the orientation distribution. To have the Digital Material be a faithful replica of the real material, a set of rules were developed for determining how geometric features and their attributes could be chosen for inclusion in the Digital Material. For instance, the Digital Material itself is, to the fullest extent possible, free from mechanical modeling concepts. The user is free to operate on a

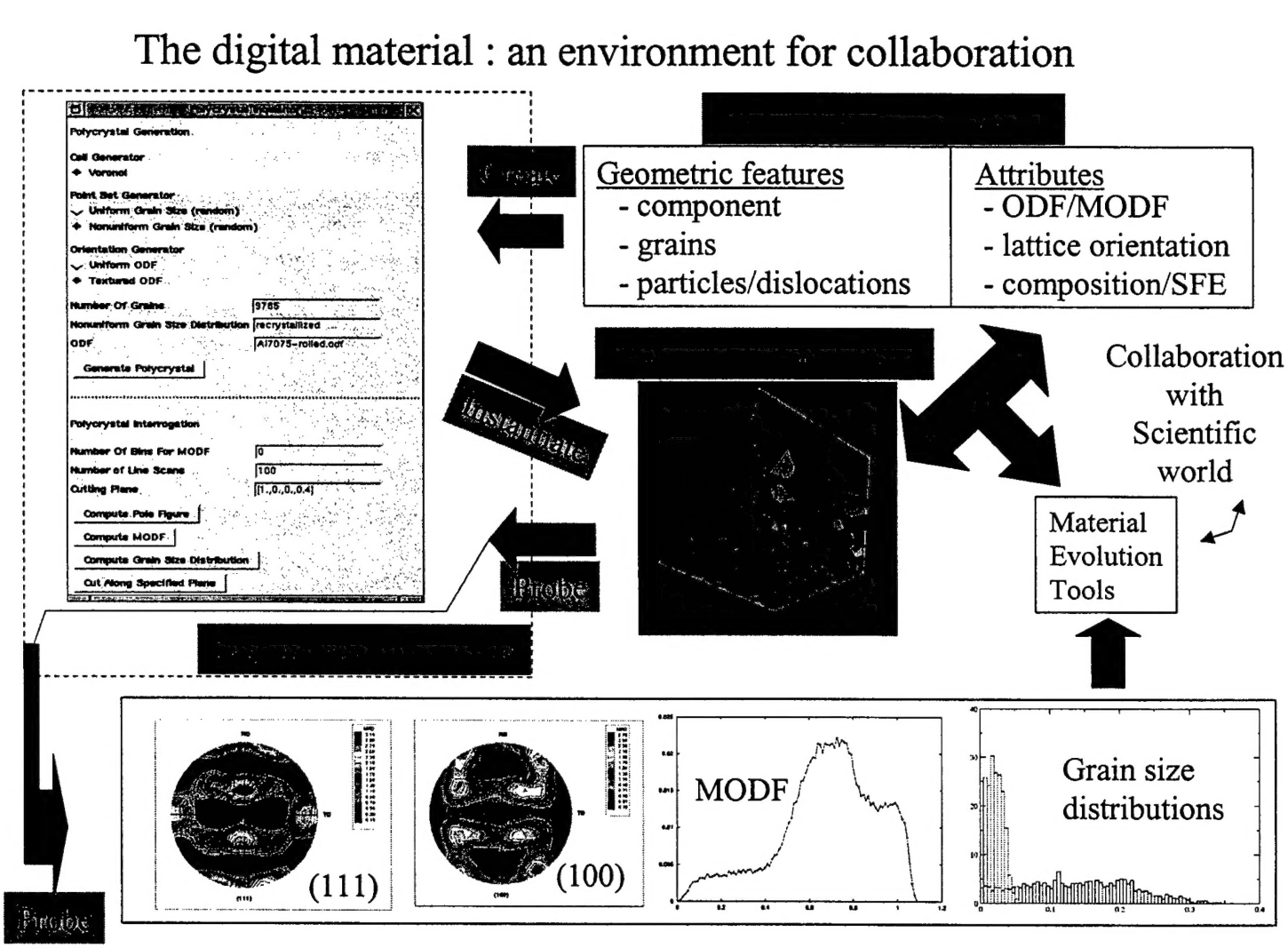

Figure 1. Schematic depicting the Digital Material and how it's created, sampled, characterized and evolved. One of the hallmarks of this representation is the lack of distinction between experimental and numerically-generated data.

sample of the Digital Material with various constitutive models, but the data that are received and returned are always primitive quantities that may be observed and measured in the real material. Clearly, a great deal of thought needs to go into the selection of the relevant internal structures that are characterized for the application of interest and the manner in which experimental data are processed for statistical relevance.

2.1 Experiments in Support of Digital Material Geometry and Attributes

For practically any process in metallic alloys the crystal structure, grain morphology and lattice orientation are of primary interest. This is the focus of the current incarnation of the Digital Material. The experimental focus of this project was on understanding the effects of the crystallographic neighborhood on fatigue crack initiation. Experiments were separated into two distinct, but closely related categories. The first sought to quantify the mechanical response of the material during cyclic loading, including the initiation of fatigue microcracks. The second sought to quantify the microstructural and mechanical state of the material, including changes that may influence the mechanical response.

For the first category, uniaxial fatigue tests were performed on polished cylindrical specimens. The loading consisted of a tensile prestrain followed by tension-compression cycling to produce colonies of microcracks. Specimens were taken from 25.4 mm thick AA 7075 T-6 plate, with their axes aligned with either the rolling direction (RD) or the transverse direction (TD) of the plate, Figure 2. All tests were conducted at a strain rate of 10^{-3} s^{-1}. Upper bounds for the pre-strain and the strain amplitude in cyclic loading were identified for AA7075 T6, as being 5% and 2.5%, respectively. Optimal loading conditions to grow distributions of microcracks were found to be about 3% pre-strain and 1% amplitude. Specimens were cyclically loaded as

indicated in Figure 3 and the stress response was measured. Specimens were fully unloaded after different numbers of cycles (1, 30, and 1000) to permit measurement of residual lattice strains by neutron diffraction. Lattice (elastic) strains were measured for a number of scattering vectors (also shown in Figure 3). As can be seen in Figure 4, the strains vary from -400 to 800 μm/m, depending on the orientation of the scattering vector and the (HKL) of the scattering plane.

After being tested, the specimen surface was prepared and observed using both optical microscopy and SEM. Figure 5 depicts a secondary electron image (with several microcracks visible) and accompanying orientation map from one of the early experiments. The loading direction of the specimen was left to right. The colors in the orientation map are related to lattice

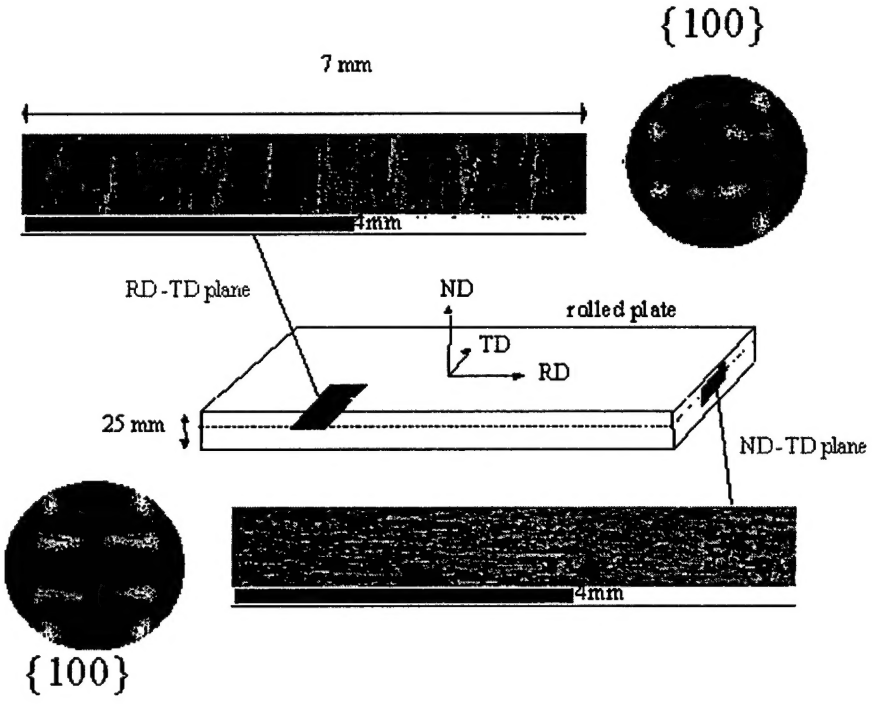

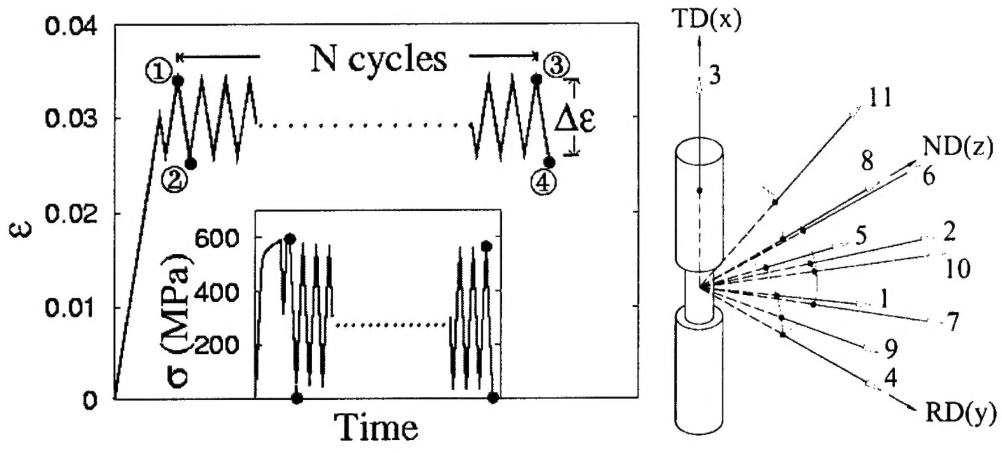

Figure 3. Applied cyclic straining cycles (left) and scattering vectors used in neutron diffraction measurements on a TD specimen (right).

The scattering vectors correspond to the families of crystallographic planes given in Figure 4.

orientation – regions of the same color indicate individual crystals. Bright green depicts regions where indexing was not possible often due to the presence of microcracks or other forms of micro-damage. As can be seen, the cracks are indeed small - much smaller than the width of the grains. For statistical relevance, the goal was to characterize the neighborhood around many microcracks. This was made possible by employing automated electron backscatter diffraction (EBSD) in the SEM. With this technique, lattice orientation was determined by indexing Kikuchi patterns produced by diffracting electrons. The process was automated to index many points a second, making it possible to characterize large areas of material in a reasonable amount of time. The intent of these investigations was to establish links between orientation, misorientation, crystal stresses, and microcrack distributions.

The orientation measurements were also employed to determine grain size and shape distributions. Based on these experimental data, probabilistic models were developed for the

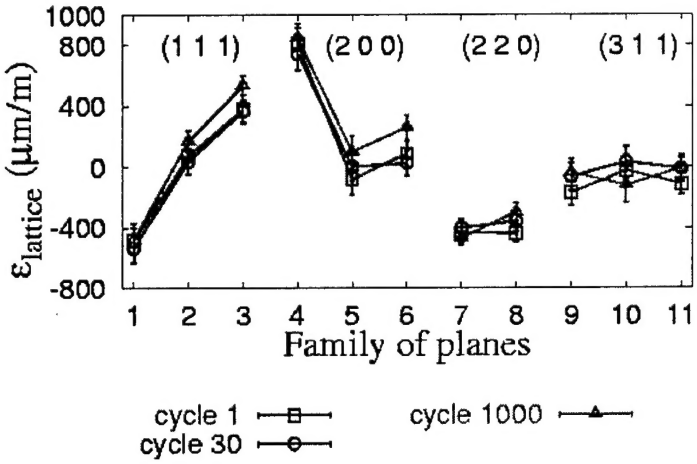

Figure 4. Lattice strains following various numbers of cycles and removal of loads. Families correspond to particular scattering vectors with orientations given in Figure 2.

grain geometry in two and three dimensions as well as for the crystallographic orientation. Techniques for generating samples from these models were implemented which allow the creation of arbitrarily many digital samples of the material, each of which is statistically representative of the measured material samples.

3.0 SAMPLE GENERATION AND PROBE TOOLS

3.1 Sample Generation Tools

Just as in physical experiments, one can extract a specimen from the Digital Material that is statistically representative of a particular material in terms of the relevant geometries and attributes. In the current case, this means the generation of an aggregate of crystals that matches various aspects of the ODF, MODF and grain size and shape distributions measured experimentally. Tesselations of a sample volume are developed, currently from Voronoi diagrams, which enable a partitioning of that volume into a set of polycrystalline grains. By

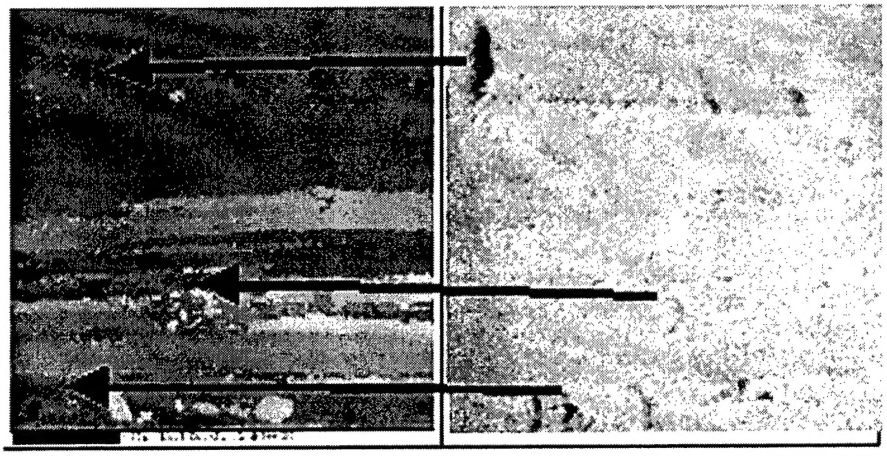

Figure 5. Secondary electron image (right) and EBSD lattice orientation map (left) of surface material from a prestrained and cyclicly loaded specimen. The loading and rolling directions are left to right. The colors in the lattice orientation map are related to lattice orientation with bright green indicating non-indexed points.

modifying the input to the Voronoi tesselation, we can construct uniform (equiaxed) grain sizes, or spatially nonuniform distributions of grain sizes, such as one might find in a partially recrystallized specimen. Additionally, orientation sampling techniques have been developed that allow us to assign crystallographic orientations to each grain based on underlying orientation and misorientation distribution functions (ODF and MODF). This process of sample generation is described in more detail in Section 4.2, below, where it is used to create samples for fatigue loading. The user interface to the polycrystal generator is depicted in Figure 1, as is the resulting Digital Material Sample.

3.2 Characterization Tools

The Digital Material sample can be probed in manners identical to those employed in physical experiments and, perhaps more importantly, in ways that are not currently possible in the physical laboratory. For example, one can create cutting planes for two-dimensional characterizations analogous to EBSD lattice orientation scans and produce pole figures, MODF profile and grain size distributions as shown in Figure 2. One can also monitor the growth of intergranular cracks much as one would through the use of replication techniques, as will be shown in Section 4.2, below. In contrast to physical experiments, one can also determine the distribution of quantities like residual stresses in a three-dimensional aggregate on a crystal-by-crystal basis, as shown in Section 4.1, below. These types of spatially-resolved stress data are currently physically unattainable but, properly calibrated with neutron diffraction results, can become extremely valuable for predicting the mechanical environment most favorable for microcrack initiation.

As described above, systematic characterization of the Digital Material is much more straightforward than in physical experiments. The accuracy will depend on things like mesh size and interpolation schemes. As will be described in the following section, the introduction of features like particles and microcracks presented distinct challenges.

4.0 MATERIAL EVOLUTION TOOLS

the usual manner. Evolution models then prescribe the material response. Simply stated, motivation, calibration and verification of material evolution models are the fundamental driving forces behind the development of the Digital Material. The Digital Material becomes the repository for the knowledge one gains related to processes such as fatigue crack initiation. The generic structure of the Digital Material allows researchers from widely varying fields to make use of it and participate in its further development.

One set of simulations that was performed was finite element calculations employing a polycrystal plasticity formulation for understanding the degradation of mechanical properties during service loading (post processing – crack initiation). This set is described in Section 4.1. Another set of finite element simulations dealt with the propagation of cracks along edges of the crystals or through the crystal interiors. These are described in Section 4.2. Underlying both of these simulation sets is a set of stochastic evolution tools described in Section 4.3.

4.1 Evolution of Intracrystalline Stresses

The objectives of this aspect of the project were: (1) to obtain distributions of inter-crystalline stresses of the studied alloys from processing, and to follow their evolution under cyclic loading; (2) to investigate the influence of intercrystalline stresses on fatigue properties; (3) to generate a statistical database (crystal stresses, elastic strains and texture) necessary for probabilistic representation within the Digital Material.

element method (each element has a distinct orientation) to represent an aggregate of crystals. Uniaxial, cyclic load histories were imposed on the aggregates following a prestraining that mimics the fabrication process.

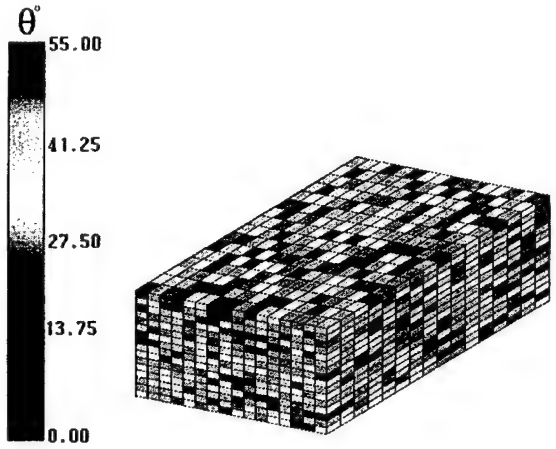

Figure 6. Finite element polycrystal showing lattice orientations assigned from sampling of the ODF residing in the Digital Material. The angle, θ, is a scalar measure of the orientation of each crystal relative to the plate directions, RD, TD and ND.

Cyclic analyses of AA7075 T6 were performed using the finite element method using the mesh shown in Figure 6. In this formulation 4096 crystal orientations were taken from the ODF and used to initialize a 16x16x16 block of brick elements. The aspect ratio of the elements reflects the measured grain geometry. The virtual specimen was then loaded in an identical manner to the experiments discussed in Section 2.1, with the axial stress component in each

interactions. The distribution of strains was returned to the digital material as part of its state description.

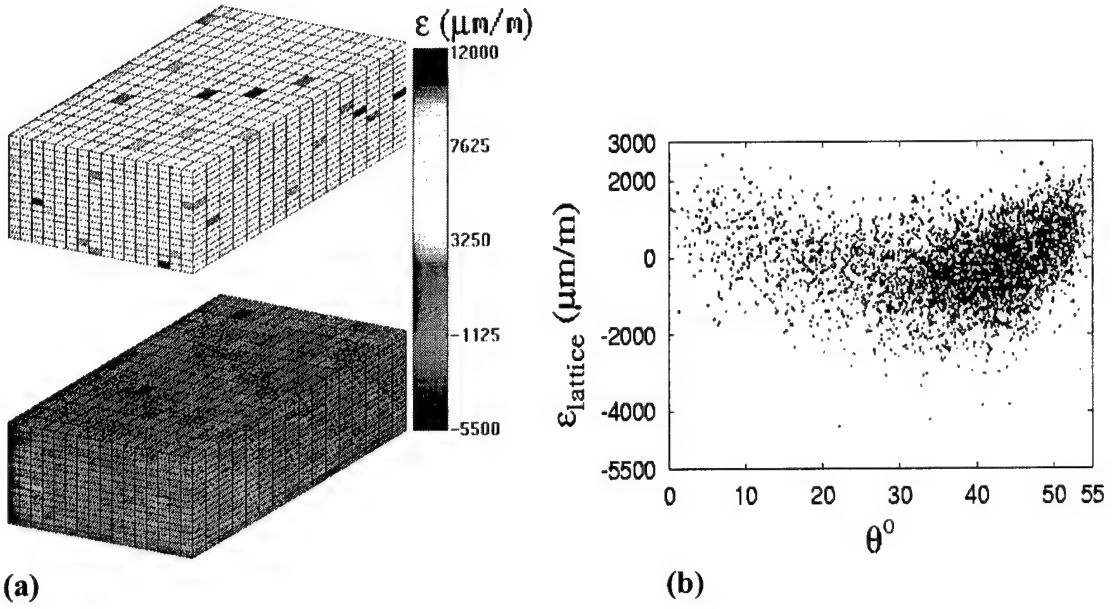

Figure 7. (a) Axial lattice strains corresponding to the peak load (top) and unloaded (bottom) states of a cyclic loading history shown as points 3 and 4 in Figure 3. **(b)** Distribution of axial lattice strain as a function of θ after unloading from the final loading cycle.

The experimental observations summarized earlier regarding the occurrence of microcracks indicate two important trends: (1) formation and growth of cracks are favored at some locations and not others, presumably due to the combined influences of crystal state (condition), the local loading environment, and the intrinsic variability that exists in these quantities; and (2) the initiation site of the microcracks frequently is associated with constituent particles. Each of these observations points to the need to resolve the polycrystal more finely than has been done to date if one is to better understand the origin of the microcracks.

4.2 Fatigue Crack Initiation Simulations

Current fatigue crack growth simulations usually involve introducing a small crack at an assumed critical location. Finite element analyses are then used to observe how the propagating crack grows and affects the residual strength of the component, and how the component will ultimately fail. Unfortunately, this approach does not give insight into when and where cracks actually initiate and grow to a detectable size.

The above approach considers a component to be represented as a continuum; however, metallic materials are heterogeneous collections of grains. Each grain in turn is a collection of various atoms and dislocations. The macroscopic homogenization smears the details of the smaller scale that determine when and where cracks will initiate. To consider the influences of each scale without explicitly modeling every atom for a large component, a multi-scale approach was employed using the Digital Material environment. Multi-scale modeling allowed details at the smaller scale to be used to enhance the larger scale without explicitly modeling the smaller scale [7]. Modeling at the polycrystal scale of a metallic material by itself can give insight into critical location and conditions for cracks to initiate. Conducting a statistical series of polycrystal simulations can create a database of information about changes in constitutive behavior due to crack initiation between grains. This database can then be used to inform finite elements or integration points in a model of a full component of changes in constitutive properties as damage accumulates.

element software package developed by the Cornell Fracture Group especially for fracture simulations and analysis. Crack initiation along the grain boundaries was observed under monotonic and cyclic loading as the cohesive elements began to open and fail.

Geometric models of aluminum microstructure were created using Voronoi tessellations [11]. The grain material was modeled by assigning individual statistical realizations of the material model chosen to each grain. With each grain having individual properties, grain boundaries naturally arose in the model. To define the properties and response of the grain boundaries a cohesive zone model was implemented. Due to the arbitrary angles of the grain boundaries, both normal and shear responses were considered through a coupled cohesive zone model to allow for mixed mode cracking.

Discussed in the following sections are the use of cohesive zone models to describe grain boundaries, the process for creating statistical samples of aluminum microstructure, and observed results from polycrystal simulations.

4.2.1 Grain Boundary Decohesion

There are many mechanisms that can lead to the initiation of micro-cracks in a polycrystal. For example, fatigue leads to the formation of slip bands within grains, which can lead to shear cracks; a corrosive environment can facilitate the failure of grain boundaries due to oxygen embrittlement. This investigation focussed on the decohesion of grain boundaries.

the strength and toughness of the grain boundaries. The CZM also served as a criterion for initiation of intergranular cracks. The grain boundaries were allowed to decohere after reaching a critical normal or shear stress or a combined transmitted traction, thus gradually initiating a crack. Once a critical opening was reached a true microcrack formed. An advantage of using such a model was that initial cracks were not arbitrarily introduced at the beginning of a simulation. Instead, cracks naturally occurred due to the heterogeneous stress field throughout the sample caused by the geometry and statistical variations in properties.

CZMs are traction-displacement relationships originally used to describe the damage that occurs in the plastic zone ahead of a crack [8]. In the present case the damage represented by the softening portion of the CZM was used to describe the decohesion of the grain boundaries. The implementation available in FRANC2D/L, includes independent normal and shear cohesive models as well as a coupled model. The coupled cohesive zone model (CCZM) was adapted from a model developed by Tvergaard and Hutchinson [12], where the normal and shear components of the traction, t, and displacement, λ, were combined into a single measure, Figure 9. A key characteristic of the relationship was the area under the curve, G_c, which represented the critical energy release rate.

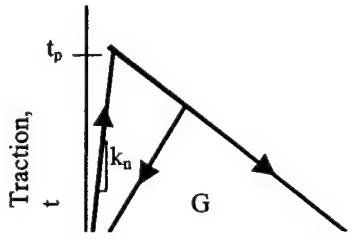

The opening and sliding displacements were normalized to the relative critical displacement values, δ_n^c and δ_t^c, at which the separation was considered a true crack in pure Mode I and II. When the value of λ reached 1 there is complete decohesion of the grain boundary and formation of a grain boundary microcrack. When a grain boundary encountered unloading, the CCZM followed the path shown in Figure 9. Upon reloading of the grain boundary after softening has occurred the CCZM followed the unloading path back to the softening portion of the curve. This resulted in full closure of the grain boundary. Grain boundary damage was seen through the reduced stiffness of the reloaded grain boundary.

4.2.2 Creation of Statistical Polycrystal Models

In a physical sample of aluminum there are more factors contributing to which grain boundaries will fail and how far a microcrack will propagate than just the relative strength and stiffness of the grains and grain boundaries. The geometry and distribution of properties increase the complexity of the polycrystal response. Therefore, statistical representations of the aluminum microstructure were created and tested.

Creating a polycrystal sample began with defining the geometry of the grains. This was done using a Voronoi tessellation. Polygons were created from a random set of initiation points. Each polygon then represented a grain as outlined by Arwade [11]. The average size of the grains was held to observed measures from electron back-scattering pattern scans (EBSP)

to be a separate realization of the material model. For orthotropic material models, an orientation was also assigned to each grain. These orientations were sampled from an orientation distribution function (ODF) created from orientation data collected through EBSP scans.

Once grain properties were assigned, orientation and property mismatch led naturally to grain boundaries along the polygon edges. With the grain boundaries located from geometry and material mismatch, interface elements were placed and assigned CCZM properties. In these simulations the parameters describing the CCZM were determined to either be the same for all grain boundaries in the sample, or to vary from boundary to boundary. For example, for the orthotropic models parameters were varied based on the misorientation angle, θ, across the grain boundary according to $\theta = \beta_1 - \beta_2$ Figure 10. Assuming that G_c varies with the angle θ , the area under the CCZM varied according to $G(\theta) = G_{avg} + \Delta G \cos(4\theta)$. G_{avg} was the average value of the critical energy release rate and ΔG determined the range of values.

The form of G was chosen based on a Fourier expansion of spherical harmonics. In 3D any periodic function can be written using a Fourier expansion of spherical harmonics of which the present case is a 2D degenerative form. Holding the normal of each grain to be along the (100) direction forces cubic symmetry for a FCC crystal. This results in the cos 4θ(or ψ) form term used here.

The CCZM can be described using several parameters. However, only 2 are independent. To isolate variation in the model to just G_c, the values of k_n and δ_n^c were held constant for all

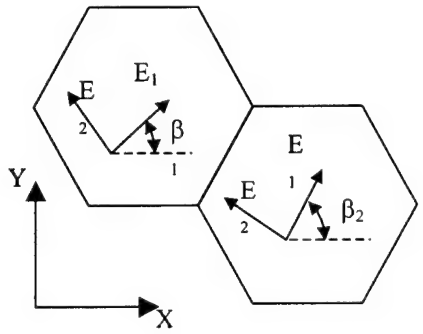

Figure 10. Orientation of neighboring orthotropic grains relative to global coordinate system. The misorientation angle, τ, is defined as the difference between the two orientation angles, β_1 and β_2.

The sensitivity of the generated sample to material properties and distributions was examined through a parametric study. Parameters varied included the tessellation used, grain material model, grain material parameter values and ranges, grain boundary parameter values and ranges. Details of simulations conducted and a discussion of the results can be found in [14].

4.2.3 Simulation of Fatigue Crack Initiation in Polycrystal Samples

Results discussed here are for the grain geometry, boundary conditions and applied displacement loading history shown in Figure 11. The tessellation shown contained 100 grains with an average size of 10 μm. For this simulation the model was constrained in the Y-direction along the bottom edge and in the X-direction on the vertical sides. Individual results will be shown for the points indicated on the loading history, Figure 11b. The grain material was modeled using Hill orthotropic plasticity, with the primary average yield stress equal to the average grain boundary strength. The average grain material properties for the Hill material model and CCZM

parameters are shown in Table 1. The implementation of the Hill yield criterion in FRANC2D/L was limited to perfect plasticity and plane stress. Due to the orthotropic model each grain was assigned an orientation angle varying from 0 to 360 degrees. This angle determined the angle between the global X-axis and the primary axis of the grain. The grain properties were then allowed to vary from grain to grain. Property values were allowed to vary ± 5% as shown in Table 1. The CCZM parameters chosen resulted in the average peak combined strength of the grain boundaries being equal to the average primary yield stress of the grains. This allowed some of the grain boundaries to reach their peak and begin softening, initiating fatigue cracks, before the grains began to yield and absorb all of the damage to the polycrystal.

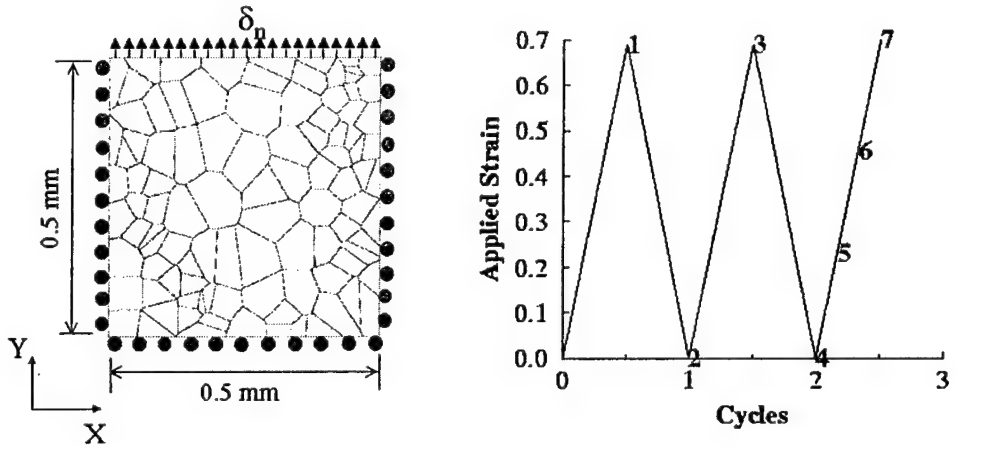

(a) (b)

Figure 11. (a) Boundary conditions and loading of polycrystal sample. (b) Loading history, applied strain percent.

Table 1. Grain Material and CCZM Properties

Grain Material		CCZM	
Type	Elastic-Plastic, Orthotropic (Hill)	G_{avg}	250 Pa m ± 5%
E_1	72,000 MPa ± 5%	ΔG	100 Pa m
E_2	40,000 MPa ± 5%		
σ_{yld1}	500 MPa ± 5%	Resulting t_{pavg}	500 MPa ± 5%
σ_{yld2}	400 MPa ± 5%	K_n	4e8 MPa
σ_{yld12}	330 MPa ± 5%	δ_c	1 μm
θ	0 – 360 degrees		

macroscopic yield strain of the overall sample. Figures 12-14 show the polycrystal responses corresponding to each of the number locations in Figure 11b.

As can be seen in Figure 12a, the distribution of material properties throughout the sample resulted in a heterogeneous stress field. Examination of the deformed mesh indicated that localized damaged had occurred on the circled grain boundaries. The close up shows that the grain boundaries have elastically separated and minimal decohesion had begun to occur. This first loading resulted in softening of grain boundaries in the interior of the sample despite its being loaded below the macroscopic yield strain. The softening grain boundaries were almost

can be seen at the boundary of the sample where a triple point occurred at the boundary. Such points left slightly higher residual stresses.

Figure 13 shows the response due to the second loading and unloading. The response was similar to the first cycle. However, the decohesion of the circled grain boundaries increased. The residual stresses present at reloading and the softer grain boundaries due to the first loading also resulted in a slightly different σ_{yy} contour plot at peak loading. To be noted are the reduced stress levels around the decohering grain boundaries in comparison with the stress level in the surrounding grains. This indicates the polycrystal is shedding the load to areas that are not softening. After unloading stress concentrations were also seen at the ends of the decohering grain boundaries.

Finally, the sample was loaded to 0.70% strain. The response was captured during the loading and then at full loading. The progression of grain boundary close-ups in Figure 14 shows the grain boundaries decohereing until finally the critical opening has been reached and localized damaged has initiated. The σ_{yy} contours in Figure 14a and b initially show the decohering grain boundaries do carry some load until Figure 14c which shows the complete shedding of loaded away from the decohered grain boundaries. Also to be noted in the stress contour in Figure 14c is the stress concentration to the right of the decohered grain boundaries. This stress concentration causes local yielding within the grain. The adjacent boundaries are almost perpendicular to the loading direction making the failure mode primarily Mode II,

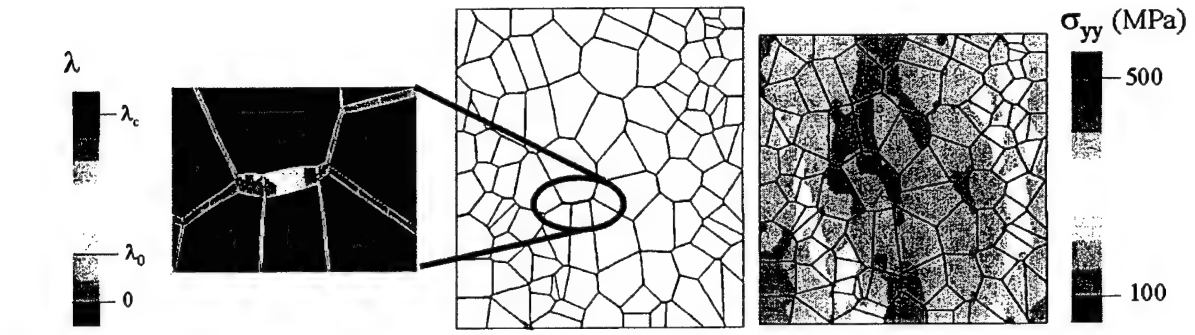

(a)

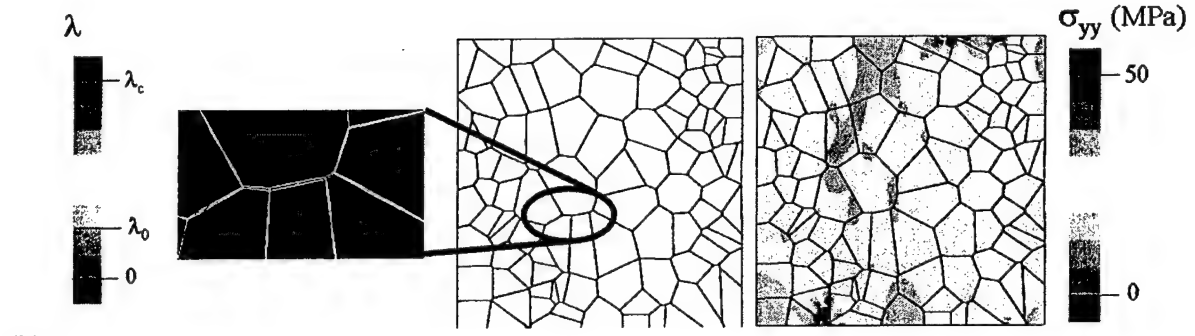

(b)

Figure 12. Polycrystal response at points (a) 1 and (b) 2 of the loading history. From right to left: σ_{yy} stress contour, deformed mesh, grain boundary opening with λ_0 and λ_c corresponding to the opening at the peak strength and the critical opening respectively.

4.2.4 Discussion

Initial simulations using bicrystal samples were conducted to observe the usefulness of cohesive zone models to describe grain boundaries. These simulations showed that cracks could be initiated without the explicit introduction of an initial crack through the use of the CCZM.

statistically assigned Hill material parameters from a range of values. The grain boundaries were assigned a statistically varying CCZM. Completed polycrystal samples were loaded cyclically to observe damage and crack initiation.

In an example shown herein, damage occurred to the sample in the form of grain boundary decohesion before any grains reach yield from macroscopic loading. Local yielding then followed due to stress redistribution caused by the decohesion process. The use of the CCZM to describe the grain boundaries allows for this type of damage to naturally occur.

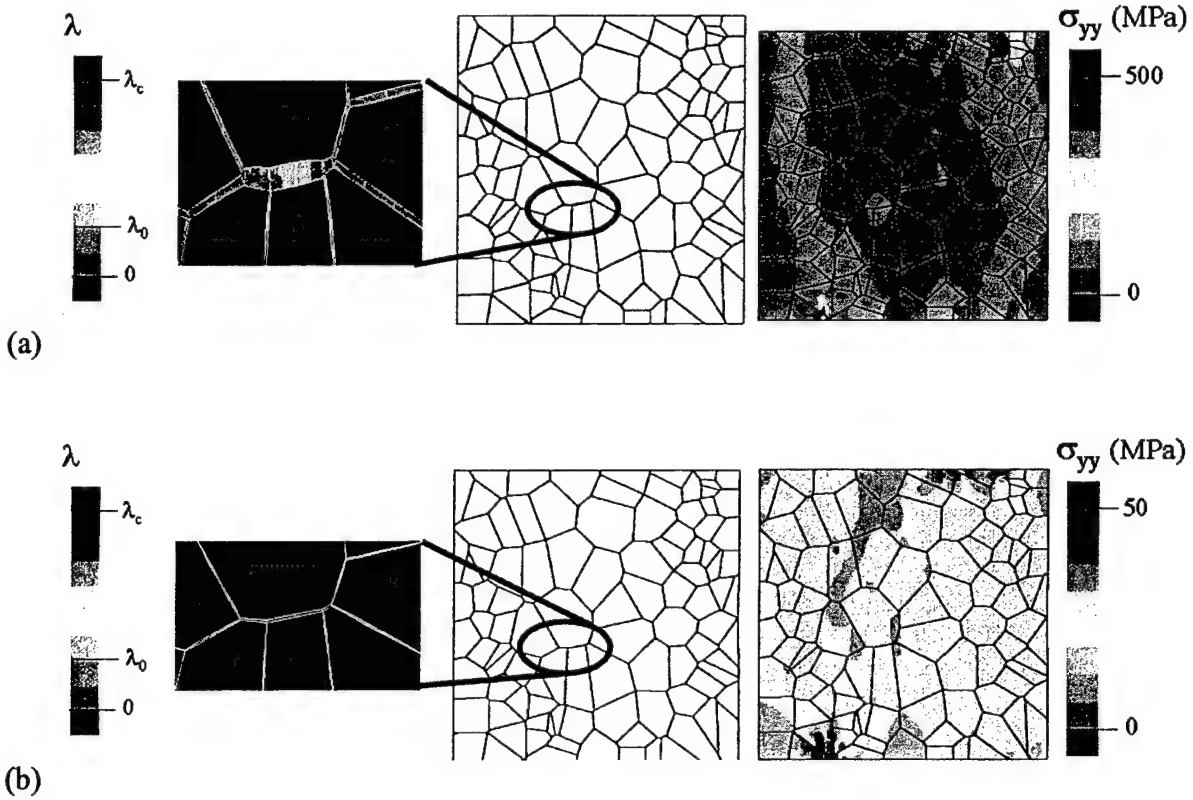

Figure 13. Polycrystal response at points (a) 3 and (b) 4 of the loading history.

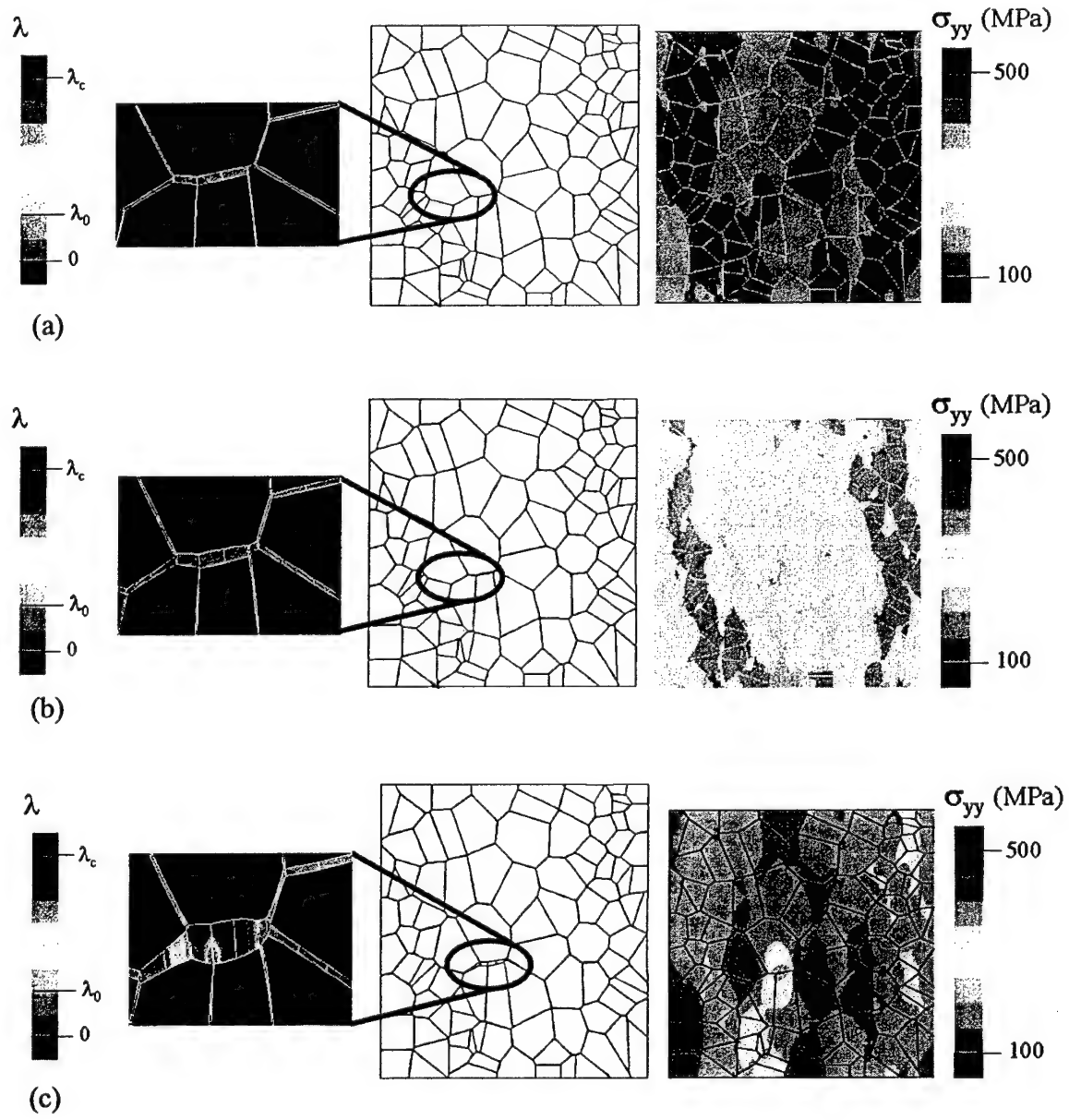

Figure 14. Polycrystal response during final loading corresponding to points (a) 5, (b) 6, and (c) 7.

influences of geometry and material properties on fatigue crack initiation. This can also be useful in collecting statistical information about where and when fatigue cracks will initiate and the residual strength of a sample. As part of a multiscale effort, this information can be used to enhance constitutive properties at larger scale and determine smaller-scale features that should be further investigated.

The CCZM can also be used to model the interface between two material where decohesion occurs. Another use within an aluminum microstructure could be the interface between hard particles or inclusion and the grains. Experimental results have shown that decohesion of the particles does occur and can be a large influence on the initiation and propagation of fatigue cracks. Modeling of particles in a statistical representation of an aluminum microstructure and the use of CCZM to describe the decohesion of the particles is being pursued in a related research project [25].

4.3 Probabilistic Evolution of Material Microstructure

Throughout the development and implementation of the Digital Material the investigators recognized the importance of considering the phenomenon of microscale damage accumulation in light of its stochasticity. The inclusion of probabilistic models in the analysis was in fact one of the primary goals of the work. The motivation for such emphasis uncertainty in system parameters was given by consideration of some features of material microstructures and the

in space in a fundamentally non-deterministic way. Such a polycrystal may then be acted upon by random external loads arising from such conditions as aerodynamic forces. The combination of random material microstructure and random external action results in material evolution that is random. Specifically, attributes of the microstructure, such as the stress or strain state and the damage state, evolve randomly. This motivation was supported by the illustrations of Figure 15, which show the stress field in an axially deformed polycrystal in which the elastic properties are inhomogeneous, varying from grain to grain, and the time evolution of the crystallographic orientation of a planar single crystal when subjected to random deformation.

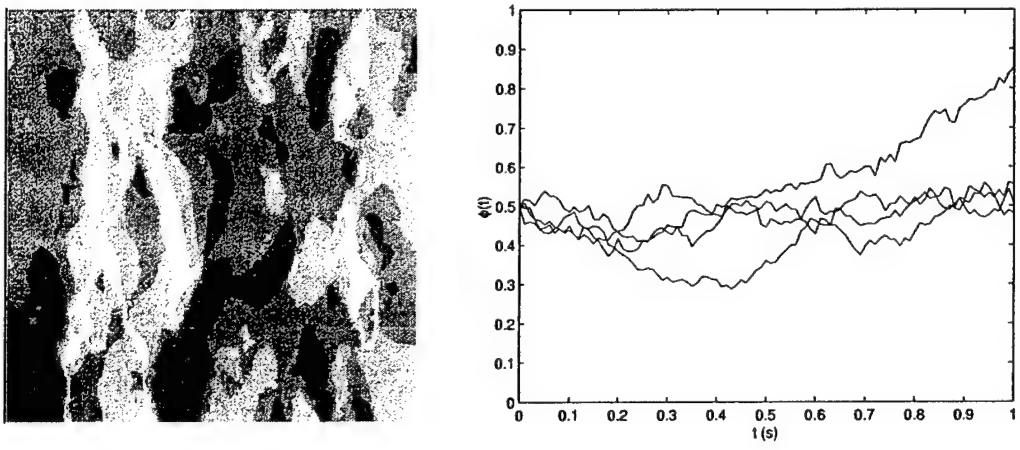

Figure 15. (Left) Stress field in a polycrystal with heterogeneous elastic properties; (Right) Time evolution of the crystallographic orientation of a planar single crystal subject to random external loads.

If realistic simulation of microscale damage accumulation is to be achieved, then the

$+ \tau$) the evolved state of the DM. The DM at each of these time instants consists of data that describe the features of the material microstructure and also the probabilistic models for these features.

This timeline of DM evolution provides the basic structure for discussion of the parts of this project pertaining to stochastic modeling and analysis. The initial state of the DM will first be described, followed by presentation of the methods of evolution, consisting of the analysis techniques themselves and the random and deterministic loads that act on the DM. The last part will be a description of the DM in its evolved state. Examples of the types of information given in each of these parts are represented graphically in Figure 17. Both simple and more complex types of random deformations are imposed on the DM, consisting either of deterministic deformation histories that are perturbed randomly or true random processes. In the evolved state of the DM certain new microstructural features are included, such as the stress state in individual crystals of a polycrystalline aggregate.

The simplistic timeline of Figure 16 can be expanded upon significantly by explicitly including the features of the microstructure that are considered as well as the types of material evolution which are simulated. Figure 18 recasts the timeline in the form of a flowchart that contains all of this information.

4.3.1 DM at Time Zero

microstructure. The probabilistic models are calibrated, when possible, to experimental data, and sample generation techniques are described.

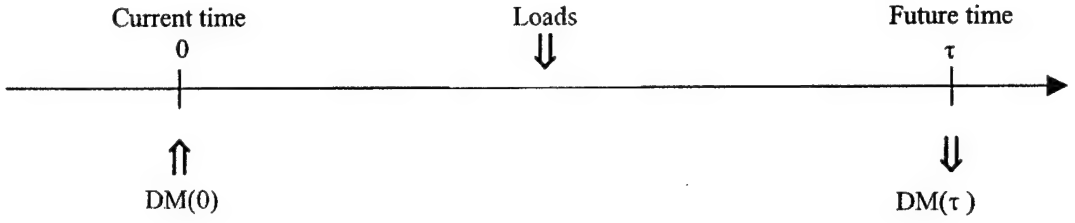

Figure 16. Schematic illustration of the evolution of the DM from an initial state to an evolved state. The DM is acted on in the evolution period by external loads that can be either deterministic or random.

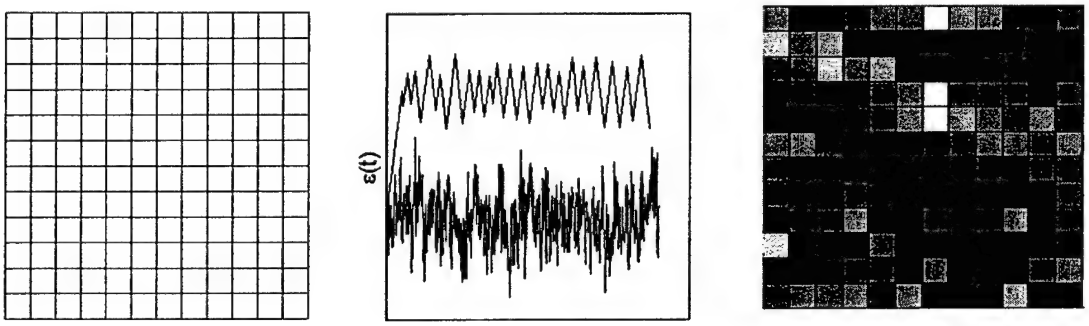

Figure 17. Initial and final states of DM with external actions. From left to right: Initial grain

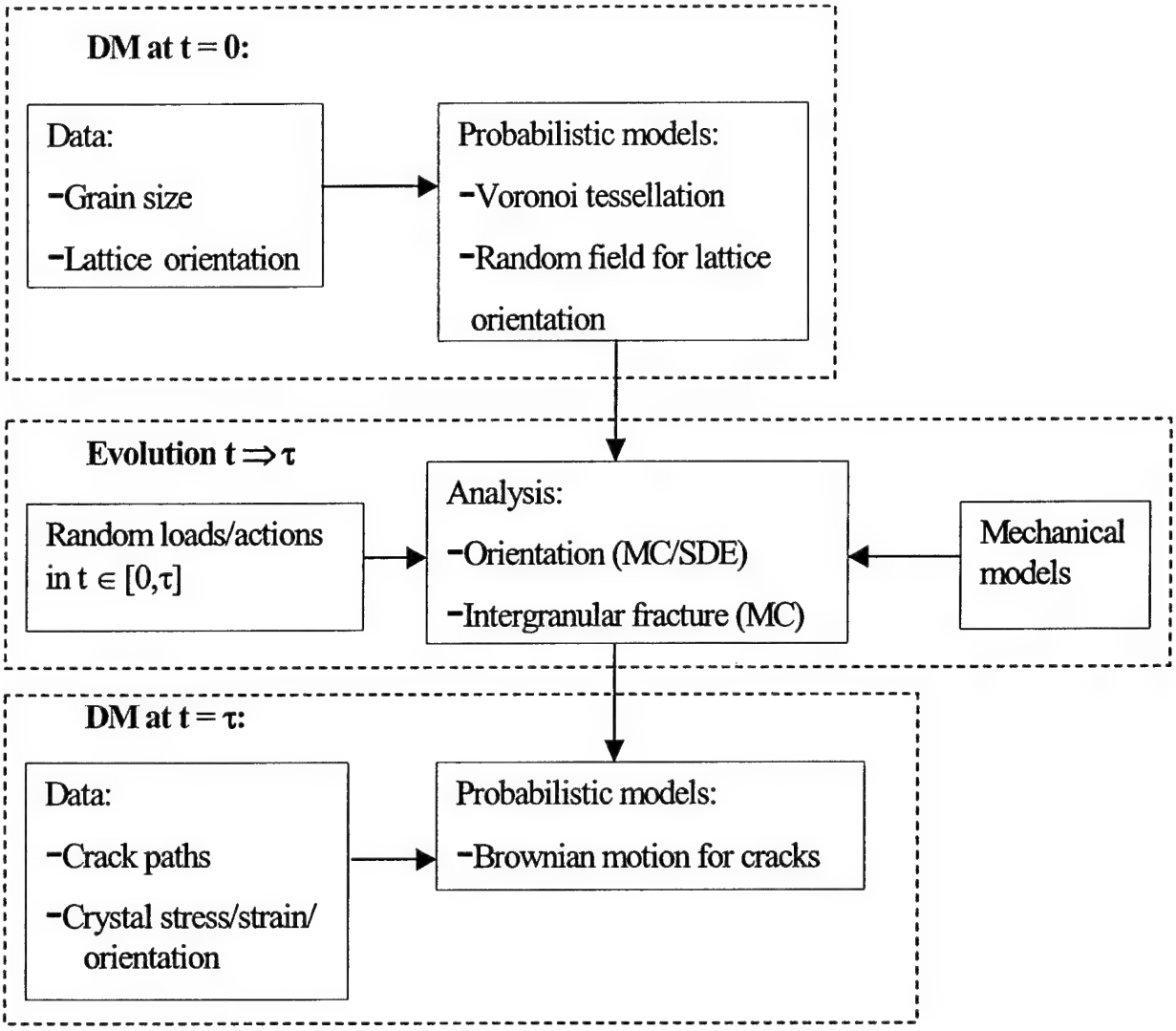

Figure 18. Flowchart of DM evolution.

The Voronoi tessellation has previously been proposed and verified as a model for

Since the tessellation is defined on the set of nuclei the real task in modeling a grain geometry is to model the nuclei. If the grain geometry is to be treated as random, then an appropriate model for the nuclei is a Poisson point process, which is defined in detail in [19]. In general, the grain size in a polycrystal may be homogeneous, and to model such a grain geometry, a non-homogeneous Poisson point field is an appropriate model for the nuclei. The calibration of such a point field is made through the intensity function. The intensity function describes the density of points throughout the domain of definition of the point field. Since nucleus density is inversely related to the average cell size of the Voronoi tessellation, so the intensity is inversely related to the average grain size. Thus, experimental measurements of the grain size can be used to calibrate the intensity function of the underlying Poisson point field. An example is shown in Figure 19 in which the intensity function varies linearly along the vertical axis of the polycrystal. This variation in the intensity function is clearly manifested in the size of the constituent grains of the Voronoi tessellation.

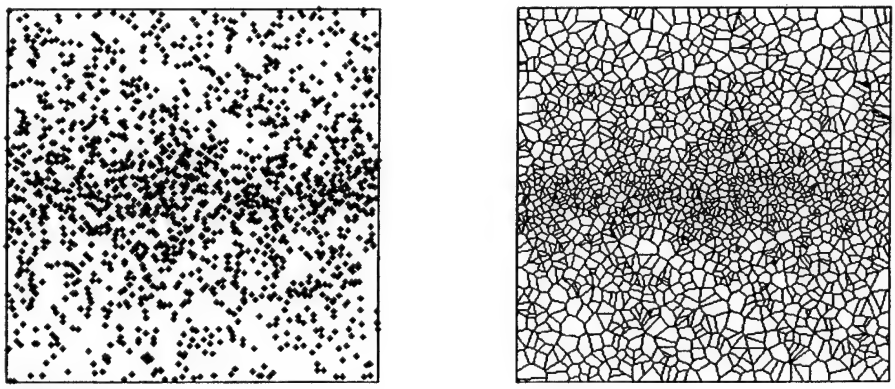

A vector random field model successfully models the crystallographic orientation in a polycrystal [15]. The random field model in its simplest form assumes that the orientation is stationary in second moment and in marginal distribution. It is, however, capable of modeling orientation fields that have nonstationary and anisotropic correlation structure when this nonstationarity and anisotropy arises from inhomogeneity in the average grain size. The random field model relies upon the assumption that the crystallographic orientation is constant within grains. The orientation is represented, for purposes of the random field model, in the form of the Euler angles. Samples of the orientation field, which is non-Gaussian and conditional upon a particular realization of the grain geometry, can be generated by translation models [20]. The random field model can be calibrated to experimental measurements both in marginal distribution and second moment properties if data are made available which provide a spatial map of crystallographic orientation throughout the domain of a polycrystal. Such data can be obtained by use of the Electron Backscatter Diffraction method [21,22]. A realization of the orientation field (Euler angle ϕ_1) upon an underlying grain geometry is shown in Figure 20, and compares favorably, except for the scale of the polycrystal which is easily adjusted, with the experimental data shown adjacent.

4.3.2 Evolution of DM

This section addresses the methods employed for evolution of the DM in three parts.

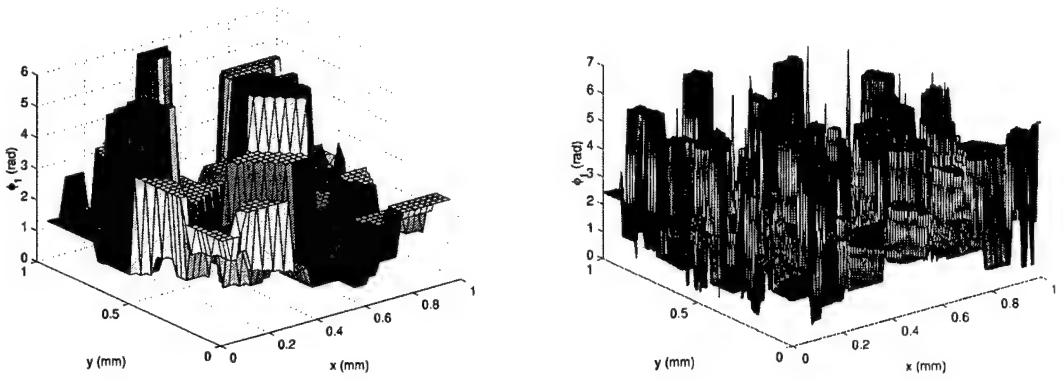

Figure 20. (Left) Realization of orientation random field (first Euler angle) upon underlying grain geometry; (Right) Experimentally measured crystallographic orientations. Measurements made by EBSD method.

the evolution of the DM are discussed which give directly the probabilistic properties of the DM at various times. These methods have the advantage of sometimes allowing analytic solutions, and of giving exact results for probabilistic features such as probability density functions. These methods have the drawback of being applicable to a relatively small number of problems, and of yielding no information regarding the evolutionary properties of individual samples of the DM. Lastly, Monte Carlo (MC) techniques for the DM evolution are described. MC techniques are advantageous in that they can be applied to a broad variety of problems, and describe the evolution of individual samples. These techniques, however, require that features such as the probability density function (pdf) of microstructural features be estimated from a large number of generated samples. Such generation can be time consuming, and the estimates obtained can be only approximate.

4.3.2.1 External Actions

Realistic simulation of the evolution of the DM has two prerequisites, appropriate models for the mechanical behavior of the material, and knowledge of the loads, motions, and deformations that act on the material, driving its evolution. These loads, motions and deformations are here referred to as external actions upon the system. The stochasticity of the DM system arises in three possible ways. The system parameters, crystallographic orientation for example, may be considered random. If this is the case, then even a deterministic action will result in non-deterministic output of the system. If, on the other hand, the system parameters are assumed to be deterministic, random external actions results in non-deterministic system output. It is also possible to have a combination of random effects, in which the system input is random as well as are the system parameters. Here, the system parameters are consistently considered to be random, but both deterministic and random external actions are considered. External actions are specified in the current work in terms not of forces, loads, and stresses, but rather as applied deformations. These deformations can be two or three-dimensional.

The stochastic actions used in this thesis consist of random time histories that give the time varying value of some parameter of the applied deformation, such as a component of the strain tensor or a component of the velocity gradient tensor. These time histories can be modeled as random processes that are here assumed to be weakly stationary, with, perhaps, an initial transient. The processes are specified by their second moment properties and marginal

frequency content consists of a single frequency, and all cycles have identical amplitude. For a random record, two methods are used for quantifying the frequency and amplitude content of the record for purposes of comparison with a deterministic record. Algorithms have been developed [24] for identifying within a random time history individual cycles along with their period and amplitude. When such algorithms are applied to a realization of a random time history, histograms of the cycle period and amplitude are obtained. Example histograms are given in Figure 21. Once the cycles have been identified average values of the cycle period and amplitude can be compared with the period and amplitude of a deterministic cyclic reference time history.

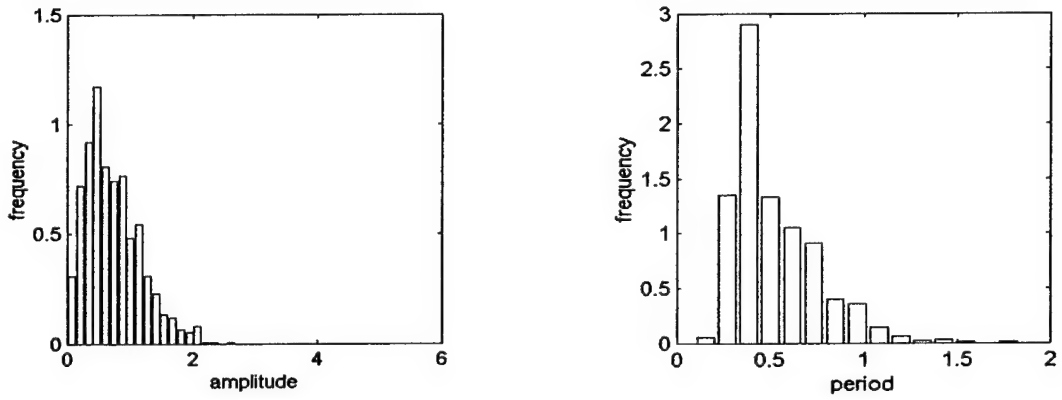

Figure 21. Histograms of cycle amplitude and period as obtained by processing a realization of a random process by the rainflow cycle counting method. The average values obtained from histograms such as these can be compared to the amplitude and frequency of deterministic cyclic records.

content of the record and the variance of the record. The peak or average value of the spectral density can be compared to the frequency of the deterministic record, and the variance can be comapared to the amplitude of the deterministic record.

4.3.3 Evolution of Probabilistic Models

For a deterministic problem the simulation of the system evolution involves tracking the values of system parameters and output. When the system under examination is stochastic, however, the evolution of the probabilistic features of the system must be determined. Examples of such probabilistic features include the pdf of system parameters or a correlation function of a random field that describes part of the system. In some cases the evolution of these probabilistic features can be analyzed directly. For example, if a stochastic differential equation has been derived which governs the evolution of a microstructural feature such as the crystallographic orientation, it may be possible to derive an equation which describes the evolution of the probability density function of the microstructural variable. If the governing stochastic differential equation is a diffusion equation, then a Fokker-Planck equation governs the evolution of the pdf of the microstructural variable.

A Fokker-Planck equation can be derived for the pdf of the scalar orientation of planar polycrystal with two slip systems and solved by the finite difference method. The direct solution for the evolving probabilistic rule of a microstructural variable by methods such as the Fokker-Planck equation is desirable because of its efficiency and accuracy. It has the disadvantages, however, of being applicable to only a relatively restricted class of problems, and also provides no information about particular sample paths of the evolving parameter. The overall behavior of the orientation system is that crystal orientations tend to drift towards one of two equilibrium

points, which are located at 0 and $\pi/2$ for the case of axial deformation. If the axial deformation is a random process with positive mean and small noise component, the probability mass drift is dramatically towards 0. If, on the other hand, the noise component is large relative to the mean of the axial deformation process, orientation probability mass is driven nearly equally to all equilibrium points of the system, Figure 22.

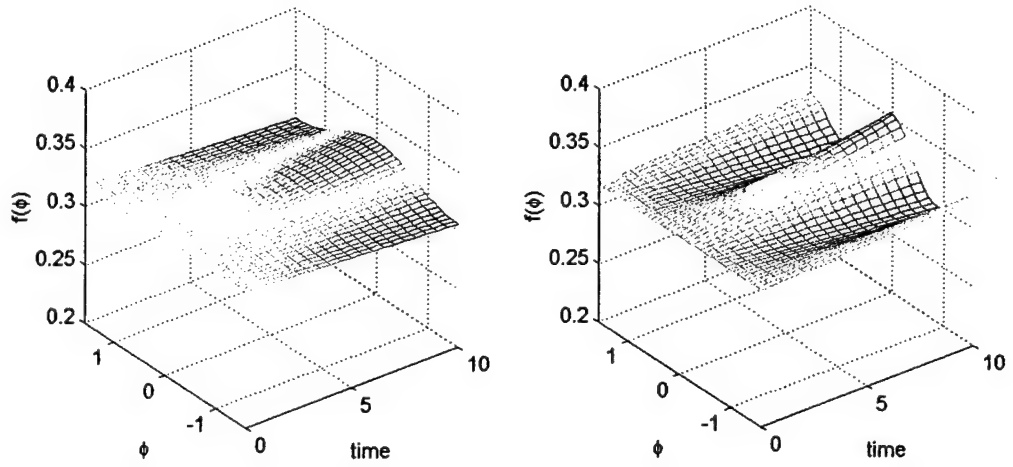

Figure 22. Solutions to the Fokker-Planck equation for the orientation of a planar crystal with two slip systems. On the left, the system is driven by an axial deformation with positive mean value and small noise component. On the right the driving force has the same mean value but significantly larger noise component.

4.3.4 Monte Carlo Simulation of Polycrystal State Evolution

It is not possible to obtain analytic solutions for the evolution of polycrystal parameters such as

developed by other [24] and so brief descriptions are given here. The two techniques are the material point simulator (MPS) method and the finite element (FE) method.

In the MPS method, the Taylor assumption is employed to significantly simplify analysis of the polycrystal state evolution. An external deformation is specified in the form of the velocity gradient tensor, and every component crystal of the polycrystal is assumed to undergo exactly this deformation. The evolution of the polycrystal is computed numerically according. The crystal parameters that are solved for in the analysis are the crystallographic orientation in terms of the Euler angles, the crystal stress tensor, the crystal total strain tensor, and the crystal elastic strain tensor. The MPS method of polycrystal analysis has the advantage that the Taylor assumption allows computationally efficient solution for the evolving microstructural parameters of the problem. The most significant disadvantage, however, is that the solution does not depend upon the arrangement of the grains in the polycrystal. It is therefore impossible to investigate the spatial characteristics of the solution. An example of such a spatial characteristic would be spatial correlation of the crystal stress components. In order to capture such spatial effects, the FE method is used.

In the FE method the polycrystal is discretized into a finite element mesh in which each polycrystal is represented by a single finite element. The polycrystal comprises, as with the MPS analyses, 1,728 grains. Each of the grains is modeled as a cube, and the polycrystal is a 12 x 12 x 12 arrangement of these cubic grains. Instead of directly specifying the velocity gradient of the deformation, as is done with the MPS analyses, boundary conditions are applied to the FE model. The applied deformations are uniaxial, Because the polycrystal is inhomogeneous and intergranular compatibility must be maintained, the deformation of each grain differs from that of its neighbors. This variability in the deformation of individual grains, combined with the

inhomogeneous material properties present throughout the polycrystal, results in spatially varying random response parameters such as crystallographic orientation, crystal stress and crystal strain.

4.3.5 Intergranular Crack Growth

While the majority of effort in the current work has been devoted to the modeling and analysis of microstructural features such as grain shape, crystallographic orientation, crystal stress and crystal strain, it is possible to attempt some crude analyses of the intergranular fracture problem in polycrystals. Models for intergranular fracture toughness [15] are now applied to determine the trajectory of an intergranular crack propagating through a polycrystal. The model polycrystal is a realization of the random grain geometry and orientation random field. The analysis procedure consists of the following steps:

- Generate a realization of the polycrystal geometry.
- Conditional upon the grain geometry, generate a realization of the orientation field.
- Select a crack initiation site at intersection of GB and polycrystal boundary.
- Determine homogeneous trajectory -- crack trajectory which would result in a homogeneous material of the same geometry and subject to the same boundary conditions.
- Advance the crack tip along successive GB segments according to either the minimum deviation or minimum misorientation criteria.

of the crack propagation across the polycrystal sample along with the homogeneous trajectory. The homogeneous trajectory is trivial to compute in this case of a square polycrystal subjected to uniaxial deformation.

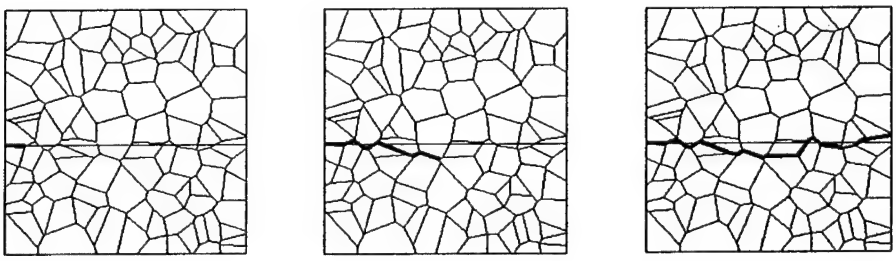

Figure 23. Propagation of an intergranular crack through a simulated polycrystal.

4.3.6 DM at Time τ

The tools for evolution presented in the previous chapter are capable of generating large amounts of data regarding the state of the DM at various time instants. Statistics of these data can be computed. Such statistics provide insight into the evolution of the DM, and also, in certain cases, suggest appropriate probabilistic models for features of the evolved microstructure. In this section some results regarding the probabilistic features of the evolved material are presented. The features considered are the crystal stress and strain and intergranular crack paths. In the case of intergranular crack paths, a probabilistic model is proposed which is able to generate realistic samples of intergranular crack paths without generating a sample grain geometry.

symmetry with respect to the loading axis. Figure 24 shows that the stress tends to be positively correlated along the loading direction, and negatively correlated in directions transverse to the loading axis. The figure illustrates this by showing a neighborhood of grains, that is, a grain (marked by the x) and each of its neighbors, and indicating by hatching the sign of the correlation between the loading direction stress in each of the neighbors and the loading direction stress in the central grain. The magnitude of the correlation is quite small, on the order of 0.20, however, the symmetry and structure of the correlation is clear. Information regarding the correlation structure of the polycrystal stress field should, in the future, be useful for developing an extended random field model that includes not only the crystallographic orientation but also the crystal stress and strain.

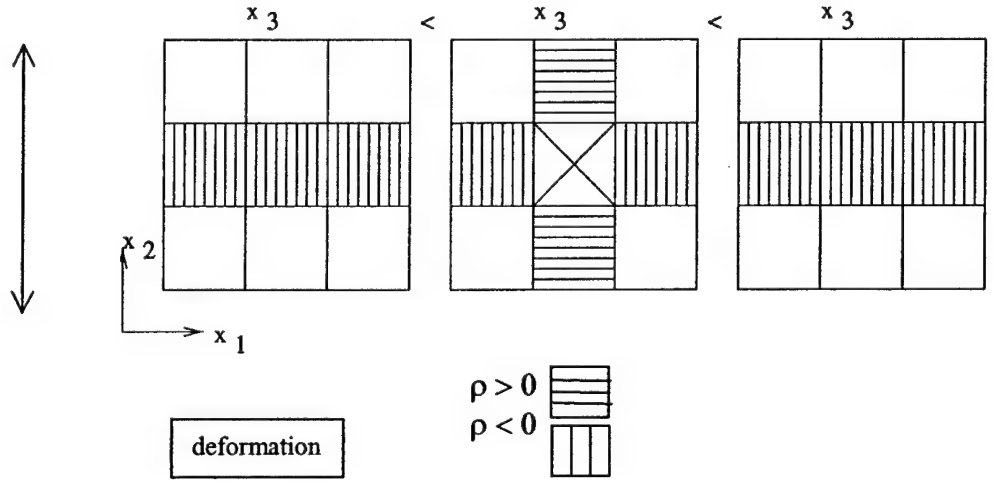

Figure 24. Schematic illustration of induced spatial correlation structure in polycrystal that has been deformed cyclically in the x_2 direction.

linearly with propagation distance. This linear increase of variance is known to be a property of the Brownian motion process that suggests that intergranular crack trajectories can be modeled by a Brownian motion process. Both the time step and rate of variance increase are related to the average grain size in the underlying polycrystal. Even by assuming a constant time step in Brownian motion sample generation the rate of variance increase can be matched exactly. Realizations of the calibrated random process agree qualitatively well with the crack trajectories determined from realizations of polycrystal grain geometries, Figure 25.

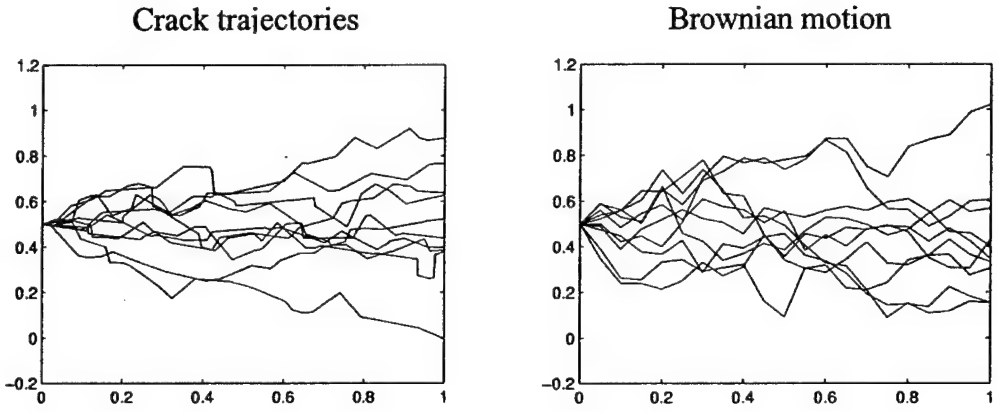

Figure 25. (Left) Intergranular crack trajectories calculated based on realizations of the underlying grain geometry. (Right) Realizations of a Brownian motion process calibrated to match the variance of the simulated crack trajectories.

REFERENCES

[1] DeJong, H.F., "Thickness Direction Inhomogeneity of Mechanical Properties and Fracture Toughness as Observed in Aluminum 7075-T651 Plate Material," Eng. Frac. Mech., vol. 13, 175-192, 1980.

[2] Suresh, S., Vasudevan, A.K., and Bretz, P.E., "Mechanisms of SlowFatigue Crack Growth in High Strength Aluminum Alloys: Role of Microstructure and Environment," Met. Trans.A., vol. 15A, 369-379, 1984.

[3] Otsuka, A, Tohgo, K, and Matsuyama, H., "Fatigue Crack Initiation and Growth Under Mixed Mode Loading in Aluminum Alloys 2017-T3 and 7075-T6," Eng. Frac. Mech., vol. 28, 721-732, 1987.

[4] Li, P, Marchand, N.J., and Ilschner, R., "Crack Initiation Mechanisms in Low Cycle Fatigue of Aluminum Alloy 7075-T6, " Mat. Sci. Eng. A., vol. A119, 41-50, 1989.

[5] Zhang, Y.H. and Edwards, L., "The Effect of Grain Boundaries on the Development of Plastic Deformation Ahead of Small Fatigue Cracks," Scripta Met., vol. 26, 1901-1906, 1992.

[7] Myers, C. R., "Digital Material: a Framework for Multiscale Modeling of Defects in Solids", contribution to the Proceedings of the Material Research Society Meeting, Fall 1998.

[8] Dugdale, D. S., "Yielding of Steel Sheets Containing Slits," Journal of the Mechanics and Physics of Solids, Vol. 8, 1960, pp. 100-104.

[9] Bittencourt, T. N., Wawrzynek, P. A., Ingraffea, A. R., and Sousa, J. L., "Quasi-Automatic Simulation of Crack Propagation for 2D LEFM Problems," Engineering Fracture Mechanics, Vol. 55, No. 2, 1996, pp.321-334.

[10] James, M. A., "A Plane Stress Finite Element Model for Elastic-Plastic I/II Crack Growth," Ph.D. Thesis, Kansas State University, 1998.

[11] Arwade, S. R., "Probabilistic Models for Aluminum Microstructure and Intergranular Fracture Analysis," M.S. Thesis, Cornell University, 1999.

[12] Tvergaard, V. and Hutchinson, J. W., "Relation Between Crack Growth Resistance and Fracture Process Parameters in Elastic-Plastic Solids," Journal of the Mechanics and Physics of Solids, Vol. 40, No. 6, 1992, pp.1377.

[13] Ingraffea, A. R., Grigoriu, M., Dawson, P., and Miller, M., Probabilistic Simulation of Fatigue Crack Initiation Annual Progress Report, Cornell University, Ithaca, NY, 2000.

[14] Iesulauro, E., "Decohesion of Grain Boundaries in Statistical Representations of Aluminum Polycrystals," M.S. Thesis, Cornell University, Ithaca, NY, 2001.

[15] Arwade, S.R. Probabilistic Models for Aluminum Microstructure and Intergranular Fracture Analysis. M.S. Thesis, Cornell University, Ithaca, NY, 1999.

[16] Arwade, S.R., M. Grigoriu, A.R. Ingraffea, and M.P. Miller. "Crack growth in stochastic microstructures." in "Stochastic Structural Dynamics" Proceedings of the 4th International Conference on Stochastic Structural Dynamics. B.F. Spencer and E.A. Johnson eds. Notre Dame, IN (1998).

[17] Preparata, F.P. and M.I. Shamos. Computational Geometry: An Introduction. Springer-Verlag, New York (1985).

[18] Stoyan, D. Stochastic Geometry and its Applications. Wiley, Chichester (1995).

[21] Adams, B.L. "Orientation imaging microscopy: Application to the measurement of grain boundary structure." Materials Science and Engineering A, A166:59-66 (1993).

[22] Mika, D.P. Personal communication (1997).

[23] Rychlik, I. "A new definition of the rainflow cycle counting method." International Journal of Fatigue, 9:119-121 (1987).

[24] Marin, E.B. and P.R. Dawson. "On modelling the elasto-viscoplastic response of metals using polycrystal plasticity." Computer Methods in Applied Mechanics and Engineering, 165:1-21 (1995).

[25] Dodhia, K. "Simulations of Crack Initiation in Aluminum Alloys with Inclusions", M.S. Thesis, Cornell University, Ithaca, NY, 2002.